2015

Polyethylene Glycol and Silica Coatings of Bismuth Nanoparticles: Synthesis, Characterization and Whole Serum Compatibilities

Victor Emilio Benavides-Montes
Portland State University

10.15760/honors.162

Polyethylene Glycol and Silica Coatings of Bismuth Nanoparticles: Synthesis, Characterization and Whole Serum Compatibilities.

by

Victor Benavides-Montes

An undergraduate honors thesis submitted in partial fulfillment of the

requirements for the degree of

Bachelor of Science

in

University Honors

and

Chemistry

Thesis Adviser

Dr. Andrea Mitchell Goforth

Portland State University
2015

ABSTRACT:

Cancer is responsible for about one fourth of mortalities in the United States daily, however, early diagnosis and treatment raised the five year survival rate since the 1970's. The usage of X-ray contrast agents (XCAs) has been instrumental in the diagnosis of tumors, but the field still calls for an improved modality in XCAs, such as safe, affordable, lower dosage and targeted XCAs. Useful XCAs must be capable of avoiding the reticuloendothelial system (RES) through an increased circulation half-life time ($t_{1/2}$), therefore, "evasive" nanoparticle shells have been previously constructed and studied. Researchers have demonstrated an increased $t_{1/2}$ with the use of molecules such as polyethylene glycol (PEG) and silica. Evasion of RES and an increased $t_{1/2}$ is primarily attributed to the decreased surface charge and robustness of said shells. Additionally, these properties prevent aggregation and foster further chemical modification for a targeting modality of XCAs. The following work aims to demonstrate a comprehensive synthesis and characterization of bismuth nanoparticles (BiNPs) enveloped by either silica or PEG. A qualitative approach using ^{1}H-NMR and FT-IR strongly suggests said coatings on BiNPs. TEM images suggest a PEG coating was formed while TEM and EDS confirms silica coatings of BiNPs. Preliminary trials of these materials in whole mouse serum advocate silica coated BiNPs are capable of sustaining their integrity in whole serum for at least 3 hours whereas PEG coated BiNPs degrade before 12 hrs. Through an optimized synthesis of either material, conjugation of proteins on surfaces should introduce the targeting component of BiNPs.

TABLE OF CONTENTS **PAGE**

1. INTRODUCTION:

a. Cancer and Current Contrast Agents

In 2015, cancer is expected to claim approximately 590,000 lives, making it the second leading cause of death in the United States yet, since the 1970's, the five year survival rate of cancer's at all sites of the body has increased to 68 percent.[1] This increase in life expectancy can be attributed to both earlier diagnosis and treatment; therefore, pursuing new methods of early diagnosis will greatly reduce the risk of death by cancer. Cancer's that are dependent on the vasculature system can be diagnosed and treated earlier if a targeted vascular contrast agent can be composed. Currently, clinically approved iodine based agents such as iopamidol, iohexol and iodixanol (Figure 1) are capable of visualizing the vascular and urinary tract, yet, their small molecular identity calls for a high dosage. Furthermore, while most iodine based XCAs are safe, this class of XCAs have demonstrated complications such as renal failure, nephropathy, anaphylaxis or allergic reactions, which constitute a death rate of 1.1-1.2 deaths per million contrast media packages distributed between 1999 and 2001.[2]

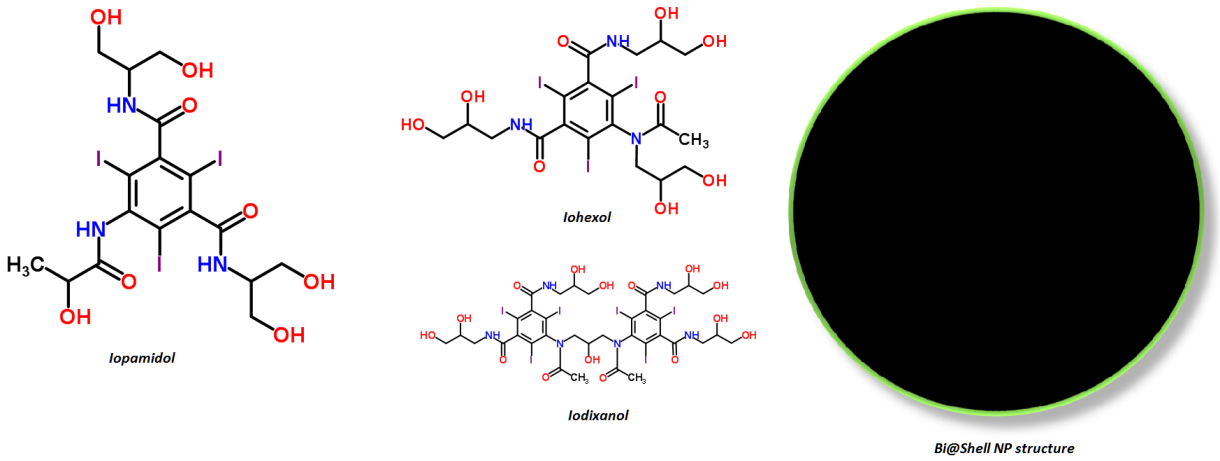

Figure 1. Iodine based agents are dependent on X-ray opaque molecular iodine (about three X-ray opaque atoms per molecule), these individual molecular structures are dwarfed in size by the proposed Bi/shell nanoparticle. A ~76nm core contains ~6 million Bi atoms (all ideally X-ray opaque) per nanoparticle (image not to scale).[3]

The introduction of new contrasting agents based off dense X-ray attenuating cores and higher atomic numbered (Z) elements such as Aurovist (gold nanoparticles) demonstrate both the improvement in contrast and lower dosage required through a dense X-ray opaque inorganic core, an attractive quality in site directed X-ray imaging. [4] However, the high cost of gold can present a practical challenge, discouraging the use of highly valued inorganic metal based XCAs. Thus, the need for an affordable, safe, and lower dosage contrast agent motivates the steps taken in this work.

b. The Reticuloendothelial System and Nanoparticle Core/Shell Structures

Most foreign entities that are introduced into the body are readily taken up by the reticuloendothelial system (RES) also known as the mononuclear phagocyte system (MPS). Without an appropriate way of "cloaking" these foreign entities, sequestration by RES (Figure 2A) is inevitable. RES functions by primarily coating said foreign entity with opsonin proteins, a molecule that triggers an immune response, facilitating sequestration of the foreign entity to the liver. This event is unfavorable if the foreign entity's (*e.g.* XCA) function requires a long or specific period of circulation time in the body, thus, "cloaking" molecules of foreign entities will prevent immediate RES sequestration (Figure 2B). Nanoparticles are attractive for specific bio-applications [5] due to their ability to avoid kidney filtration [6] and ability to avoid RES through appropriate "cloaking" chemicals. It is worth noting that it is assumed that nanoparticles with a diameter greater than 10 nm will be ideal candidates for evading sequestration by the kidneys, while nanoparticles that remain larger than 100 nm can readily be absorbed by the liver or spleen. [7, 8] Consequently, nanoparticles lend themselves for an increase in circulation half-life time ($t_{1/2}$) based on factors such as, composition of the core and coatings, surface charge, size and targeting ligand functionalization. [7, 8] Through a sufficiently large $t_{1/2}$, nanoparticles have

demonstrated the ability to target receptors of cancer growth, [9, 10] tumor growth, [11] bone tissue damage [12] and diseased spleen. [13]

Thus, it becomes evident that in order to avoid the loss of the inorganic XCA core, it must not venture alone into a physiological environment without appropriately gearing it with the capability of either avoiding RES or giving it the ability of increasing its $t_{1/2}$, which in turn, will facilitate the visualization of soft tissue.

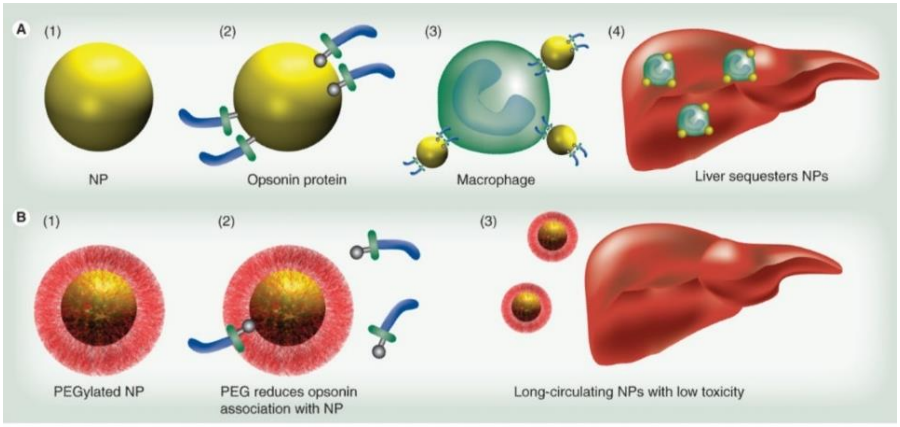

Figure 2. (A) If no "cloaking" mechanism is in place, opsonin adsorption onto the NP will greatly decrease the $t_{1/2}$ (B) unless a type of shell envelopes said NP, assisting evasion of liver sequestration (primarily through a neutral surface charge). [7]

Previous work has demonstrated an overall increase in $t_{1/2}$ by covalently linking polyethylene glycol onto the surface of a contrast platform (PEGylation). PEGylation of InAs(ZnS) quantum dots, [6] gold nanocrystals, [14] and various other platforms [7] have increased $t_{1/2}$ due to PEG's ability to neutralize the overall charge of the particle with a sufficiently dense coating, increased water solubility through the ethylene glycol repeats, and its ability to suppress particle aggregation and adsorption of opsonin proteins (Figure 2B).[7,8, 15] For these reasons, it would be advantageous to PEGylate (covalently link) or PEG coat (a non-covalent linkage) BiNPs in efforts to conceal the central core from the body's RES. Additionally, polyethylene glycol's terminal hydroxyl moieties lends itself for even further chemical modification, this ideally can enable the construction of the wanted targeted XCA. It should be noted that a PEG coating rather than a PEGylation will not foster the ideal targeting XCA and may not even sustain small changes in solvent environments. Therefore, a way to create a PEGylated BiNP should be the synthetic goal.

It is also recognized that other compounds such as silica (SiO_2) constitute favorable chemical conditions for nanoparticles in physiological environments. Silica's non-cytotoxic and robust [16] nature will prevent damage to cells and "leakage" of metallic ions into solution. Silica also imparts colloidal stability in aqueous environments via a negatively charged surface, which also prevents any silica-coated particles from coming into close contact due to electrostatic repulsions. This silica surface will also accept further chemical modifications, such as amines or thiols covalently linked to a targeting moiety or biomolecule, allowing another path towards the ultimate goal of obtaining a targeted XCA. Achieving greater biocompatibility for metallic nanoparticles, namely bismuth, through the inert silica shell, [17, 18] would present a more affordable synthetic protocol of an alternative class of XCAs composed of silica coated BiNPs.

c. X-rays and Bismuth

The use of XCAs such as barium sulfate and molecular iodinated species have existed for well over half a century. By using higher atomic numbered (Z > 18) elements as XCAs, the visualization of soft tissue and other organelles composed of smaller atomic numbered elements (*e.g.* carbon, nitrogen, oxygen, hydrogen) can be improved, as demonstrated by current X-ray radiographs (Figure 3). Therefore, by exploiting this inherent property of higher Z elements, a safer, more affordable and higher X-ray attenuating XCA can be created.

Heavy metal bismuth (Z=83), a component of the active ingredient in gastrointestinal pain relief medication (the most common being Pepto-Bismol), possesses many advantageous qualities making it an attractive candidate as an XCA. Inherent in bismuth is its minimal cytotoxicity, [3, 19, 20] making it a surprisingly safe heavy metal given both its position and the radioactive elements that surround it on the periodic table. Bismuth itself is radioactive; however

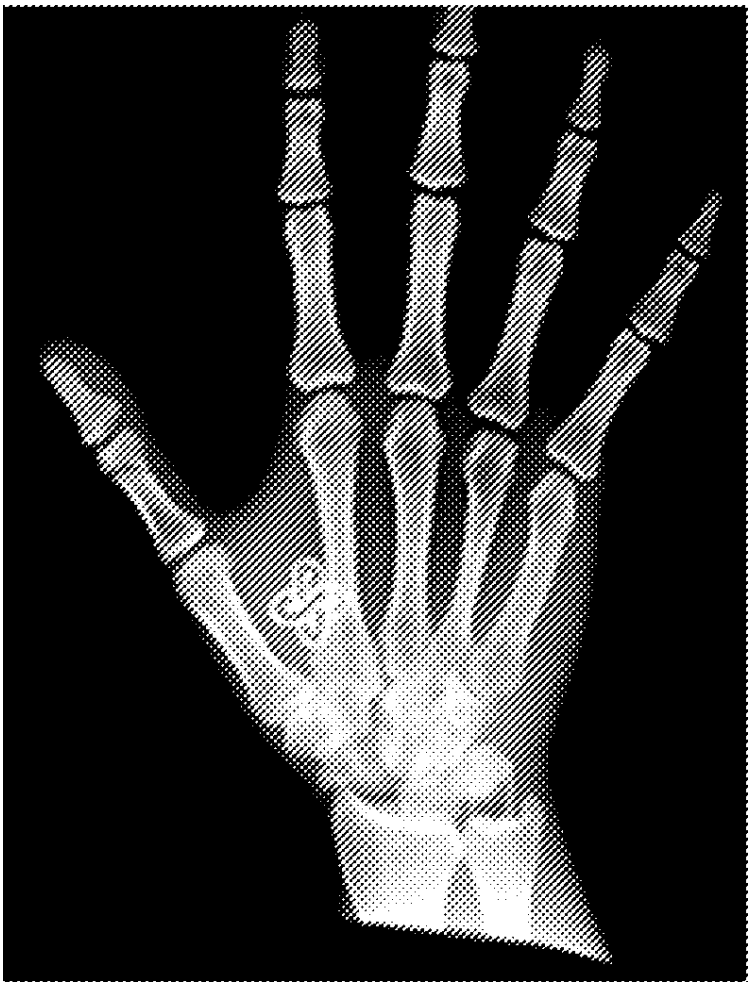

Figure 3. Material composed of higher Z elements will demonstrate greater contrast in X-ray imaging, such as the PSU logo bismuth composite. [25]

its only stable isotope, ^{209}Bi, has a half-life about 1.9×10^{19} years, [21] a period longer than the current estimated age of the universe (1.4×10^{9} years).

Due to the higher X-ray attenuation by higher Z elements, similar X-ray attenuation of iodine is observed at lower concentrations of bismuth [3, 22] which can substantially lower the dosage of contrast media if an XCA were composed of bismuth. It is also important to note the relatively low starting cost of elemental bismuth, about $8.00 per pound, [23] compared to elemental gold, costing over $17,350 per pound [24] which similar commercially available XCAs to those proposed (*e.g.*Aurovist) are composed of, potentially alleviating a practical issue for researching and producing metal-based XCAs.

Previous bismuth nanoparticles have demonstrated the ability to target (organs and disease) and/or have high X-ray attenuation/opacity. [9 , 22, 25] Thus we venture to demonstrate a simple bench-top synthetic protocol (with two potential coatings) and suitable characterization methods. For preliminary results of whether these nanoparticle core/shell structures will be able to sustain a physiologically similar environments, whole serum trials will be performed. It is postulated that

if a PEGylated nanoparticle is constructed, the material will sustain the whole serum trial, while silica coated material should also present little issue.

2. EXPERIMENTAL SECTION:

a. Materials

A PEG coated BiNP synthesis required an initial bismuth source of bismuth (III) nitrate pentahydrate (Acros Organics, 98%), a reducing source of borane morpholine complex (Alfa Aesar, 97%), polyethylene glycol-200 solvent (Alfa Aesar) and α-D-Glucose (Acros Organics) used as the particle stabilizer. Electrophoretically pure water (nH_2O) dispensed from a Millipore Milli-Q plus unit was used. NMR solvents of either D_2O (Cambridge Isotope Laboratories, 99.9%) or DMSO (Sigma-Aldrich, 99%) were used for NMR analysis to confirm the synthesis of the PEG-BiNPs.

In composing silica coated BiNPs, a bismuth precursor of synthesized BiNP concentrate from the Brown et al synthesis [3] was used. Said BiNPs were vigorously mixed with a solution of nH_2O, isopropanol, ammonium hydroxide (Stock, ~30%), and tetraethyl orthosilicate (Sigma-Aldrich).

Preliminary studies for serum compatibilities were conducted with whole serum (MP Biomedicals, Mouse, Purified).

b. Methods

A modification to the synthetic protocol established by Brown and co-workers [3] was used to construct PEG coated BiNPs: by changing the solvent to polyethylene glycol and quartering mass and volumes of reagents, PEG coated BiNPs were synthesized and purified for

characterization and further biological assays. The construction and purification of silica coated BiNPs followed much of the procedure established by Kladir et al. [26] with primary variations in quantities of volumes of the starting reagents

PEG-BiNPs were ultimately purified through centrifugation and a subsequent dialysis using dialysis tubing (SnakeSkin regenerated cellulose dialysis tubing, 10k MWCO). Every step of the purification process (centrifugation and dialysis), in both solid and aqueous liquid solutions of BiNPs, were analyzed to discern whether components of the purification were necessary. To obtain a solid, aqueous particle solutions were suspended in a volume fraction of ethanol, followed by oven drying at 150°C for at least two hours creating a solid paste-like black material (white material for silica coated BiNPs). The black material produced was then characterized via FT-IR or immediately diluted with NMR solvents for NMR analysis. However, given the reliability of eliminating water using this preparation method, the use of water suppression techniques with FT-IR (a simple subtracting of a FT-IR water scan) and NMR (an algorithm programmed into the instrument to subtract water signals) were used. Silica coated BiNPs (for both aqueous and solid material) were prepared in a similar fashion with only purification by centrifugation in a 1:1 ethanol:nH_2O solvent wash. No NMR was performed on silica coated BiNPs.

For TEM analysis, particles were directly extracted from the synthetic batch container or from dialysis tubing (aqueous solutions) and decanted straight onto a TEM copper grid (Ted Pella) and subsequently allowed to dry in the 150°C oven for at least half an hour.

c. Instrumentation

Instrumentation used to characterize the final product included a *Fourier Transform-Infrared Spectrometer* (FT-IR), a Thermo Scientific Nicolet iS10 spectrophotometer was used for a collection of signature bond stretching and a qualitative comparison of similar peaks between reagents and products. *Proton Nuclear Magnetic Resonance Spectrometry* (^{1}H-NMR), a Bruker 600 MHz AVANCE-III Nuclear Magnetic Resonance (NMR) spectrometer was used to isolate characteristic peak intensities of PEG's ethylene glycol hydrogen's at 3.6 parts per million.[7,27] A *Transmission Electron Microscope* (TEM) FEI Tecnai F-20 TEM operating at 200kV was used to visualize a final core/shell structure. Using a TEM feature, *Energy Dispersive X-ray Spectroscopy* (EDS) was performed, data collected provided an elemental analysis of the core/shell structure via the *Oxford Instruments AZtecEnergy* program. *Dynamic Light Scattering* (DLS), a Horiba LB-550 dynamic light scattering instrument and an instrumental algorithm was used to obtain a preliminary hydrodynamic radius.

3. RESULTS AND DISCUSSION:

a. PEG coated BiNPs

Material in the Bi/PEG (core/shell) configuration was characterized with various instrumentation and at different stages of the purification protocol. Control (no purification) particles in the aqueous liquid phase analyzed by FT-IR demonstrated (Figure 4) very prominent O-H stretches and H-O-H bending[28] suggesting the primary component of the sample was water. In efforts to increase the signal to noise ratio, increased scanning trials were performed, which resulted in a subtle but enhanced signal (Figure 4: trial 1). This suggests stretches associated with

a different chemical species, calling for a further degree of analysis since this data is insufficient to recommend that controls primarily hold BiNP/PEG. Oven dried particles became very difficult to work with, this was due to the high viscosity of the substance formed, a consequence of impurities that remained in solution, thus further complicating the analysis method and preventing a collection of a solid black material to analyze through FT-IR and ^{1}H-NMR. Thus, TEM and its features proved to be the best tools of analysis for these control BiNPs.

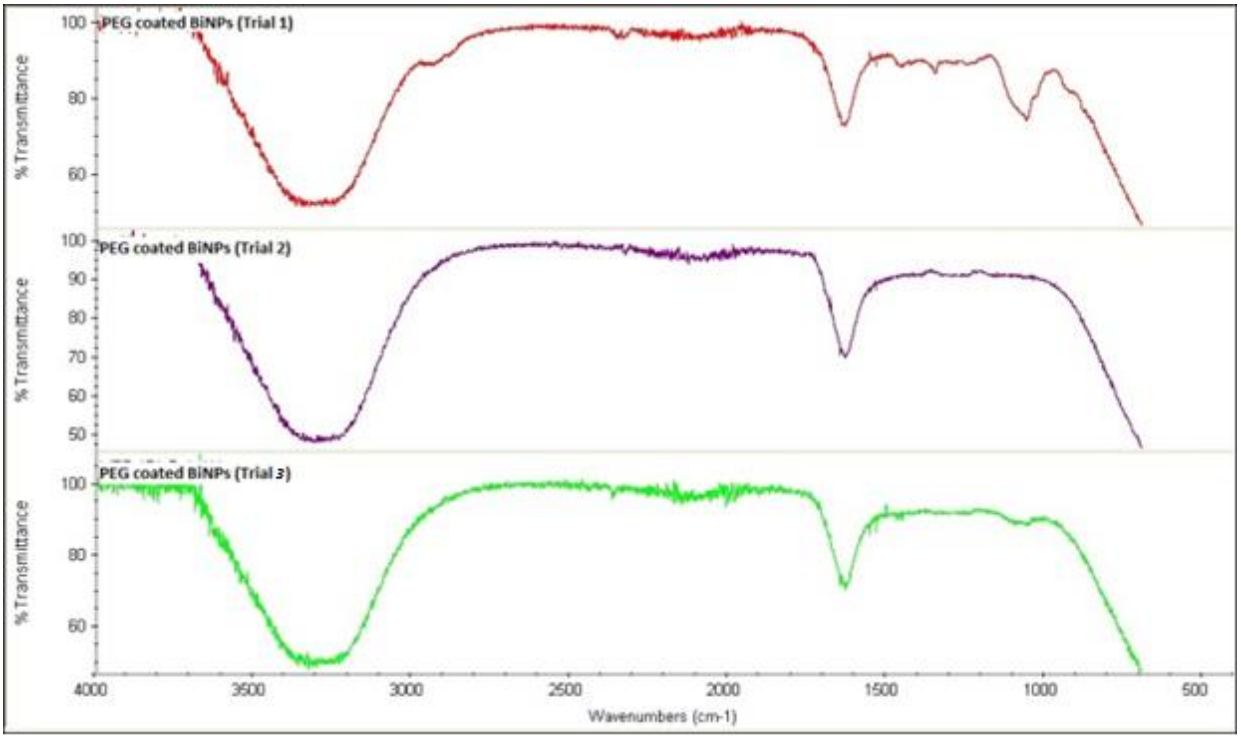

Figure 4. Control BiNPs demonstrated more peaks with an increase in scans (trial 1>trial 3>trial 2) but was still insufficient to corroborate a coating of PEG.

TEM images of control BiNP/PEG demonstrate what seems to be bismuth nanoparticles amongst synthetic debris (possibly solvent, reducing agent, or stabilizer) with a thinning layer of bismuth towards the ends of the particle (Figures 7A & 7B), this may suggest organic interactions on the surfaces of these nanoparticles, yet, this is not sufficient evidence of PEGylation or PEG coating. Nevertheless, EDS analysis demonstrates what seems to be an organic layer (PEG). Through an

EDS elemental analysis (Figure 7E), signals of both carbon and oxygen are present, alluding to the sought out PEGylated BiNP structure. It is worthy to note, through the EDS, low X-ray counts of carbon and oxygen are observed when compared to bismuth. Furthermore, the noise observed in EDS carbon and oxygen counts call for a better characterization of the material, thus a further purification (centrifugation) of the PEG-BiNPs.

Centrifuged Bi/PEG nanoparticles suspended well in ethanol for the purpose of attempting to remove as much debris as possible. These particles were oven dried very quickly (~1 minute); the remaining solid black material was subsequently analyzed via FT-IR and ^{1}H-NMR. Through FT-IR (Figure 5), a qualitative assay of prominent reagents in the reaction were compared to the final product (Figure 5: Red Trace).

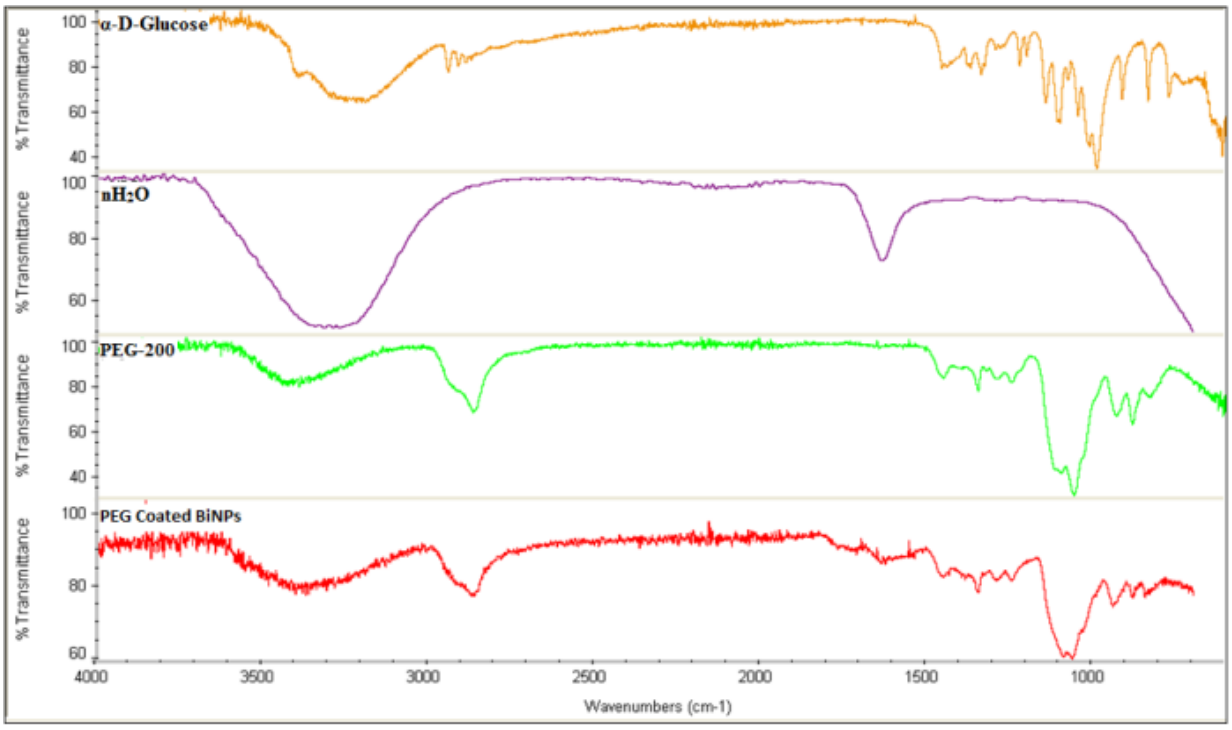

Figure 5. PEG coated BiNPs demonstrate the greatest correlation with PEG-200 through FT-IR data. All other reagents highly suggest to have little contribution to the composition of the final product.

A broad peak that extended from 3000-3600 cm^{-1} due to an alcohol (O-H) bond stretch is likely due to a trace amount of water. Peaks observed below 1500 cm^{-1} when directly traced to peaks of PEG-200 (Figure 5: Green Trace) highly suggest the primary surface of these BiNPs are coated with PEG-200. Most stretches of α-D-glucose (Figure 5: Yellow Trace) fall within the same range of PEG-200 (below 1500 cm^{-1}) or water (~1650 cm^{-1}), thus, FT-IR data is not compelling enough to suggest the centrifuged BiNPs are (Figure 5: Green Trace) do not contain glucose. Therefore, a qualitative ^{1}H-NMR assay of the reagents PEG-200 and α-D-glucose were compared to the centrifuged Bi/PEG nanoparticles.

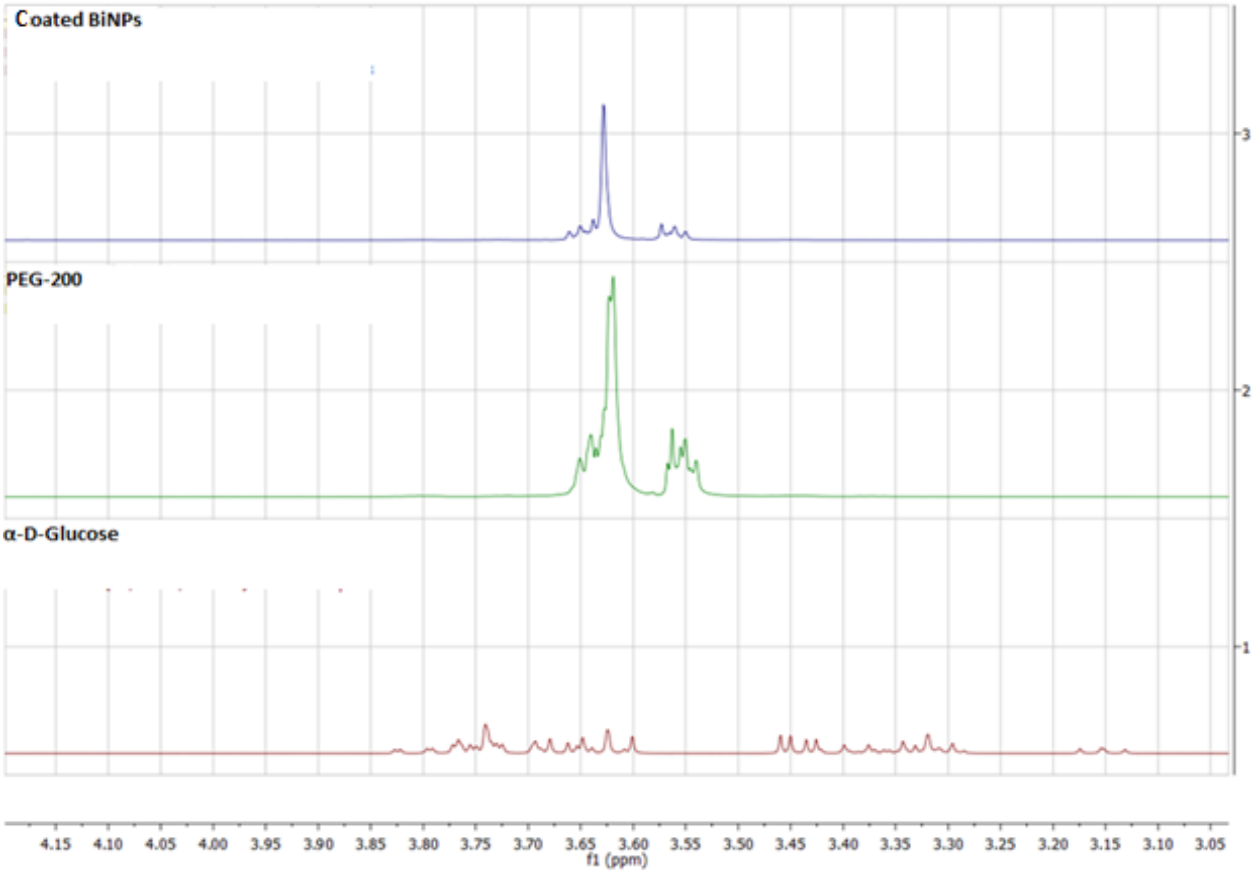

Figure 6. Coated BiNPs demonstrate a greater intensity of PEG-200-like signals, suggesting either a PEGylation or aPEG coating to the bismuth core.

The collected solid demonstrated ethylene glycol's protons at approximately 3.6 ppm (Figure 6: Green Trace), data which is in agreement with the literature [7, 27] A qualitative comparison between the final coated BiNPs (Figure 6: Blue Trace) and reagents of interest (potential coatings) demonstrate no significant quantities of α-D-glucose present on the final BiNP product. Most remarkable in these results are the peak resemblances of PEG (Figure 6: Green Trace) in the final "coated BiNPs" data. The FT-IR data in combination with the ^{1}H-NMR results strongly suggest a Bi/PEG species has been created through this synthetic protocol. However, whether a PEGylation or PEG coating has been formed to the BiNPs is still unclear. Yet, purified particles have provided good insight into the potential coordination of PEG on these BiNPs.

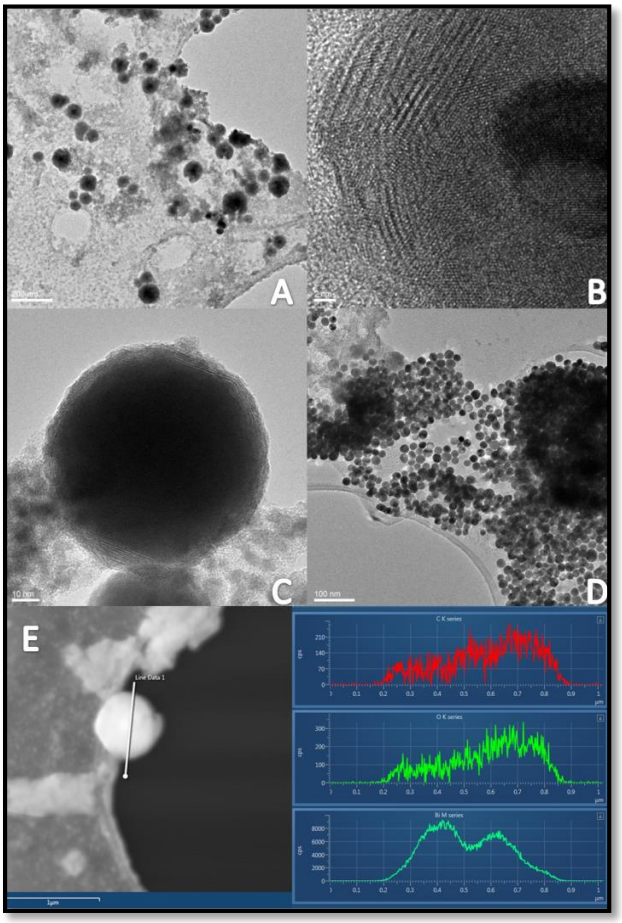

Figure 7. (A) TEM images demonstrate how controls end up with a core/shell structure with impurities, (B) a close-up of control BiNPs shows what might appear to be a core/shell structure. (E) Analysis of this sample's core/shell type structure with EDS strongly suggests the either a PEGylation or coordination to the BiNP core. (D) Particles that have been completely purified demonstrate aggregation of NPs (C) with apparently thinning shells.

Purified particles (centrifuged and subsequently dialyzed), ideally were free of any debris and thus solutions of aqueous BiNPs were directly analyzed like before, using ^{1}H-NMR and FT-IR instruments. When measured through FT-IR and ^{1}H-NMR, water was still present at very high concentrations, even after using the appropriate water suppressing techniques. The use of the oven drying preparation procedure resulted in what appeared to be absolutely no material, the glass

vial only contained trivial unappreciable quantities of black material from large volumes of BiNP aqueous solution. Therefore, the best form of analysis was again TEM. TEM images demonstrated that completely purified BiNPs contained less impurities and debris, but a greater degree of aggregation (Figure D). Additionally, a change in the surface of these nanoparticles arose. This very thin shell is different from what was observed with control BiNPs shells (Figures 7B & 7D). Previously, a dense core with a large thinning shell length (~10 nm) could be observed, after a full purification, particles appear to have smaller thinning shell length (~3 nm). This effect was observed in particles dialyzed at greater periods of time (> 3 hours) which additionally demonstrated precipitation in the vessel and through TEM, confirmed that there was indeed an aggregation of particles. This aggregation of BiNPs appears to initially occur after about two hours of dialysis (Figure 7D) strongly suggesting an issue with the final dialysis purification process. Thus, BiNPs were then dialyzed for less than two hours in order to improve the aggregation issue, which slightly helped in resolving the problem. Therefore, shorter periods of dialysis were maintained in order to keep colloidal stability in an aqueous suspension of BiNPs. The fact that the dialysis process caused precipitation/aggregation after a short period of time may indicate the actual interacting nature of the polyethylene glycol with the BiNP core was actually more coordinating (PEG coating) rather than bonding (PEGylation). This weak interaction may give rise to complications *in vivo* and *in vitro* when the particle must sustain its integrity at different pH levels, NP concentrations and ionic strength solutions. This result advocates for an alternative route to be pursued in the preparation of PEGylated BiNPs, such as the previously demonstrated sulfur bonded gold NPs synthesis. [14]

b. Silica coated BiNPs

Material in the Bi/SiO_2 configuration followed the literature established Ag/SiO_2 NPs synthetic protocol [26] yielding a white aqueous solution. This material was suspended in ethanol after centrifugation and was allowed to air dry for approximately 5-10 minutes, resulting in a white paste-like material that was characterized via FT-IR and TEM.

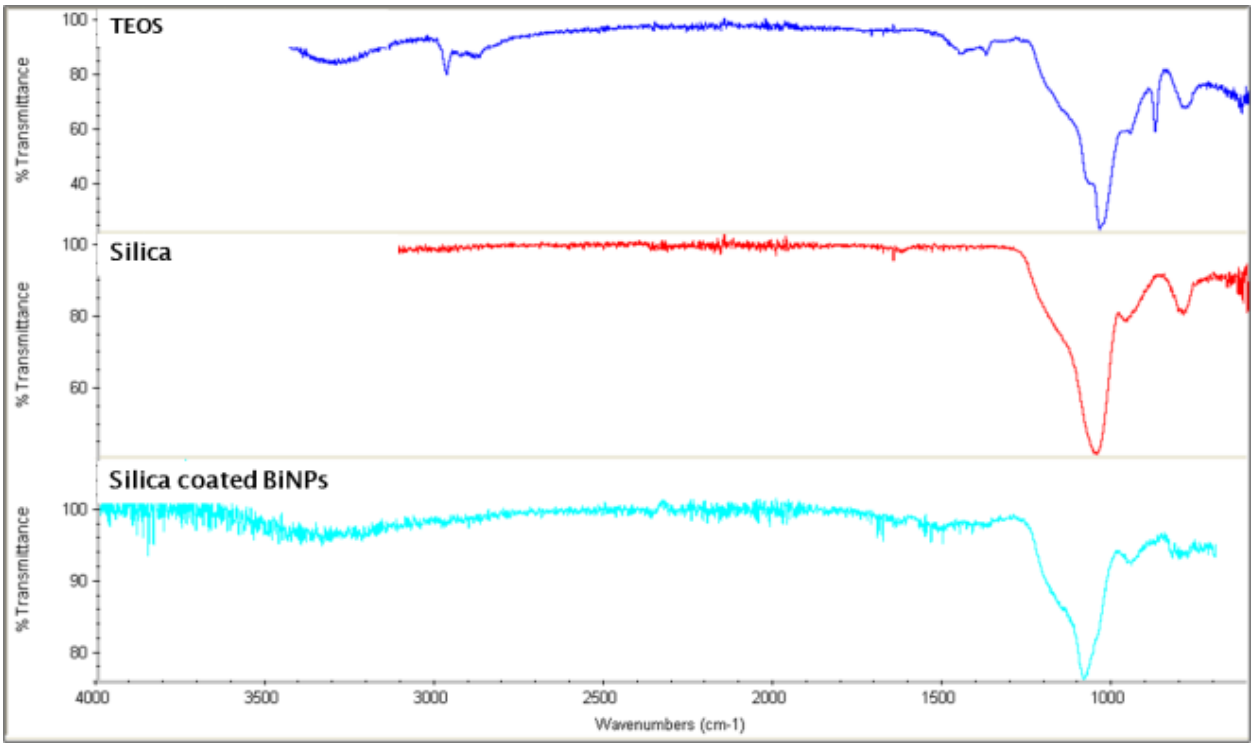

Figure 8. Characteristic peaks of dry BiNPs suggest that a shell of silica may have encapsulated BiNPs.

FT-IR data of silica coated BiNPs (Figure 8: Aqua Trace) demonstrates a prominent Si-O-Si stretch right above 1000 cm^{-1}, a small Si-O bend right above 800 cm^{-1} and a small Si-OH stretch in the vicinity of 930 cm^{-1}. Again, through a qualitative assay of reagents of interest compared to the final product, it is observed that the final products (Figure 8: Aqua Trace) stretches overlap best with silica stretches (Figure 8: Red Trace). FT-IR stretches coincide with Shokri et al's findings, [29] strongly suggesting a SiO_2 species in the final synthesized material. Through the usage

of TEM, images reveal and confirm a core/shell structure was in fact synthesized (Figure 9A). While FT-IR has alluded to the shell composition, EDS further validated the claim of a silicon-oxygen species comprising the shell of the final core/shell structure (Figure 9C).

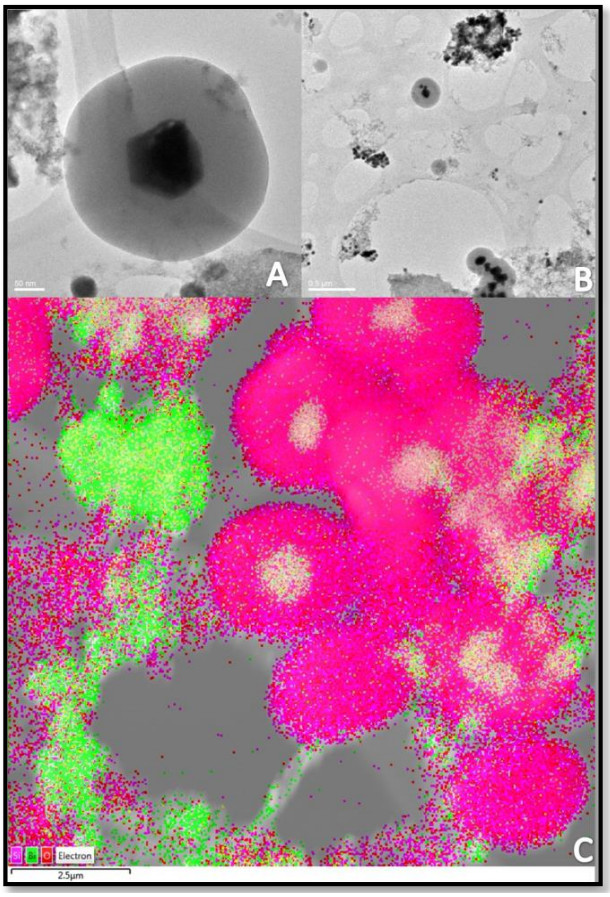

Figure 9. (A) TEM images elucidate the core/shell structure of silica coated BiNPs. However, it is apparent that while some particles are coated with some coating, not all BiNPs have been coated (B & C). (C) EDS spectra demonstrates a shell structure primarily constructed of silicon and oxygen with a core of bismuth.

However, it was noted that not all material was coated by the SiO_2 shell, which suggests a change and controlled concentrations of the current synthetic protocol must be made, specifically the BiNPs source. The apparent agglomerations of uncoated BiNPs might indicate the silica source to be a limiting reagent via the current synthetic protocol. Ultimately, an ideal synthesis should be modified to produce monodisperesed silica coated BiNPs with a high payload (a high core:shell volume ratio). It should be noted that after additional runs of the purification protocol, TEM analysis resulted in a very "clean" grid, or a greater difficulty in finding particles throughout the grid. This further endorses the need to optimize the synthesis for the future collection of more silica coated BiNPs.

c. Whole serum preliminary results

Initial trials of PEG coated BiNPs have demonstrated, through TEM images, a deconstruction of the material (Figure 10A) after twelve hours of setting the material in whole serum solution. This result demonstrated that a more dense coating or a covalently bonded form of PEG may be necessary in order to give the particle increased time of integrity in whole mouse serum. This result also suggests a weak bonding nature (likely more of a coordination) of PEG onto the surfaces of BiNP cores and may allude to a $t_{1/2}$ less than 12 hours.

Through the alternative BiNP coating, silica coated BiNPs demonstrate a good stability and the integrity of the silica spheres after three hours was maintained. This shows that Bi/SiO_2 structures can endure a whole mouse serum environment and may allude to a $t_{1/2}$ greater than 3 hours. Further whole serum assaying of both types of particles should be performed, including collecting TEM images of both particles post whole serum exposure at approximate equivalent times.

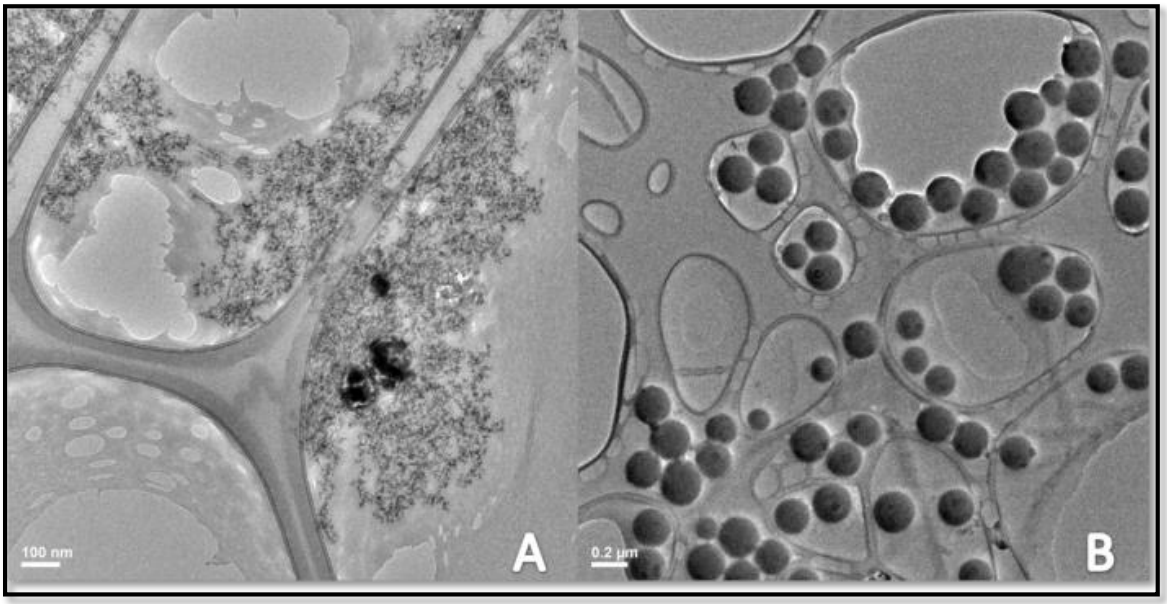

Figure 10. (A) Preliminary whole serum trials suggest a poor PEG coating of BiNPs due to their decomposition in whole mouse serum (B) Meanwhile, silica coated BiNPs appear to endure the trial.

Summary and Conclusions:

Efforts to create a better XCA have led to the synthesis of two different kinds of BiNPs with potential increased $t_{1/2}$ via molecular shells that "cloak" or are robust/inert enough to avoid RES. Control PEG coated BiNPs allude to, through TEM and EDS analysis, an organic shell composed of carbon and oxygen, strongly suggesting some type of PEG interaction with BiNPs. Upon further purification through centrifugation, a qualitative FT-IR and ^{1}H-NMR analysis makes the conclusion of a synthesized Bi/PEG more apparent via the varied synthetic protocol. Finally, PEG coated BiNPs post centrifugation and dialysis demonstrate particle aggregation (observed through TEM images) and precipitated material after performing extensive periods (> 3hrs) of dialysis. These types of BiNPs also revealed what appeared to be a thinning shell (~3 nm) where control particles demonstrated this shell to be greater (~10 nm). Whether these lengths are edges of elemental bismuth or shells of PEG is still inconclusive. It is also important to note that certain stages of the purification protocol were limiting to certain forms of analysis owed to issues with the collection of substantial amounts of material or material containing too much water. Preliminary whole serum trials suggest that the coating of PEG was insufficient to sustain its integrity after twelve hours of exposure to whole mouse serum, suggesting a potential $t_{1/2}$ less than 12 hours for PEG coated BiNPs.

Silica coated BiNPs were also successfully synthesized through a variation of a previously established method for creating silica coated silver nanoparticles. An EDS analysis reveals a coating of a Si-O species, strongly suggesting the silica species is present. TEM images distinctly demonstrate the composition of a core/shell structure. Studies using whole serum exposure demonstrate by TEM imaging that no decomposition of Bi/SiO_2 nanoparticles occured. This result is potentially indicative of a $t_{1/2}$ greater than 3 hours. Future work will continue to produce similar

particles with modifications in both syntheses to create more monodispersed BiNPs with their respective coatings, less debris formation, a higher payload and eventually an optimized synthesis. Whole serum results will be used as screenings for different coatings of BiNPs. To decrease agglomeration of particles, different steps in the purification will be used in post dialysis PEG coated BiNPs, such as decreasing the time of dialysis. A different synthesis must be created to construct a PEGylated bismuth nanoparticle. Ultimately, targeting peptides of angiogenesis receptors highly expressed in tumor vasculature of lung cancer can be conjugated onto both Bi/PEG or Bi//SiO_2 to target and isolate lung cancer at early stages.

Acknowledgements:

I would like to thank Dr.Sheng-Kuei Chiu for his incredible patience, imaging of my material and mentorship throughout all facets of this project. Dr. Anna Brown, for teaching me the appropriate methods of bench top nanoparticle synthesis and facilitating the inception of my love for nanochemistry and the element bismuth. Dr. Andrea Goforth, for believing in me enough to give me the opportunity to access her laboratory to create, learn, and pursue the questions inspired by this project and the study of inorganic chemistry. And to all the Goforth lab members that have come and gone during the years of 2011-2015, you've all made some impact in my understanding the atomic world. Finally, to all the members of the Chemistry Department that I have directly interacted with here at Portland State University, I'd like to thank you for satisfying my curiosity of the molecular world.

References:

1. American Cancer Society, 2015. Cancer Facts & Figures 2015. www.cancer.org/acs/groups/content/@epidemiologysurveilance/documents/document/acspc-036845.pdf (accessed March 23, 2015).

2. Wysowski, D. K.; Nourjah, P. Deaths Attributed to X-Ray Contrast Media on U.S. Death Certificate. *American Journal of Roentgenology* **2006,** *186,* 613-615.

3. Brown, A. L.; Naha, P. N. C.; Benavides-Montes, V.; Litt, H. I.; Goforth, A. M.; Cormode, D. P. Synthesis, X-ray Opacity, and Biological Compatibility of Ultra-High Payload Elemental Bismuth Nanoparticle X-ray Contrast Agents. *Chemistry of Materials* **2014,** *26,* 2226-2274.

4. Jakhmola, A.; Anton, N.; Vandamme, T. F. Inorganic Nanoparticles Based Contrast Agents for X-ray Computed Tomography. *Advanced Healthcare Materials* **2012,** *1,* 413-431.

5. Jain, P. K.; Huang, X.; El-Sayed, I. H.; El-Sayed, M. A. Noble Metals on the Nanoscale: Optical Photothermal Properties and some Applications in Imaging, Sensing, Biology and Medicine. *Accoounts of Chemical Research* **2007,** *41* (12), 1578-1586.

6. Choi, H. S.; Ipe, B. I.; Misra, P.; Lee, J. H.; Bawendi, M. G.; Frangioni, J. V. Tissue- and Organ-Selective Biodistribution of NIR Fluorescent Quantum Dots. *Nano Letters* **2009,** *9* (6), 2354-2359.

7. Jokerst, J. V.; Lobovkina, T.; Zare, R. N.; Gambhir, S. S. Nanoparticle PEGylation for imaging and therapy. *Nanomedicine* **2011,** *6* (4), 715-728.

8. Alexis, F.; Pridgen, E.; Molnar, L. K.; Farokhzad, O. C. Factors Affecting the Clearance and Biodistribution of Polymeric Nanoparticles. *Molecular Pharmaceutics* **2008,** *5* (4), 505-515.

9. Kinsella, J. M.; Jimenez, R. E.; Karmali, P. P.; Rush, A. M.; Ramana Kotamraju, V.; Gianneschi, N. C.; Ruoslahti, E.; Stupack, D.; Sailor, M. J. X-Ray Computed Tomography Imaging of Breast Caner by using Targeted Peptide-Lableled Bismuth Sulfide Nanoparticles. *Angewandte Chemi International Edition* **2011,** *50,* 12308-12311.

10. M, W.; Löwik, D. W. P. M.; Miller, A. D.; Thanou, M. Targeting the Urokinase Plasminogen Activator Receptor with SYnthetic Self-Assembly Nanoparticles. *Bioconjugate Chemistry* **2009,** *20,* 32-40.

11. Soudy, R.; Ahmed, S.; Kaur, K. NGR Peptide Ligands for Targeting CD13/APN Identified through Peptide Array Screening Resemble Fibronectin Sequences. *Combinatorial Science* **2012,** *14,* 590-599.

12. Zhang, Z.; Ross, R. D.; Roeder, R. K. Preparation of functionalized gold nanoparticles as a targeted X-ray contrast agent for damaged bone tissue. *Nanoscale* **2010,** *2,* 582-586.

13. Peracchia, M. T.; Fattal, E.; Desmaële, D.; Besnard, M.; Noël, J. P.; Gomis, J. M.; Appel, M.; d'Angelo, J.; Couvreur, P. Stealth® PEGylated polycyanoacrylate nanoparticles for intravenous administration and splenic targeting. *Journal of Controlled Release* **1999,** *60,* 121-128.

14. Mei, B. C.; Susumu, K.; Medintz, I. L.; Delehanty, J. B.; Mountziaris, T. J.; Mattoussi, H. Modular poly(ethylene glycol) ligands for biocompatible semiconductor and gold nanocrystals with extended pH and ionic stability. *Journal of Materials Chemistry* **2008,** *18,* 4949-4958.

15. Amoozgar, Z.; Yeo, Y. Recent advances in stealth coating of nanoparticle drug delivery systems. *Nanomedicine and Nanobiotechnology* **2012,** *4* (2), 219-233.

16. Selvan, S. T.; Tan, T. T.; Ying, J. Y. Robust, Non-Cytotoxic, Silica-Coated CdSe Quantum Dots with Effecient Photoluminescence. *Advanced Materials* **2005,** *17,* 1620-1625.

17. Li, C.; LI, Y.; Ling, Y.; Lai, Y.; Wu, C.; Zhao, Y. Exploration of the growth process of ultrathin silica shells on the surface of gold nanorods by the localized surface plasmon resonance. *Nanotechnology* **2014,** *25,* 1-7.

18. Zhang, T.; al., e. Cellular Effect of High Doses of Silica-Coated Quantum Dot Profiled with High Throughput Gene Expression Analysis and High Content Cellomics Measurements. *Nano Letters* **2006,** *6* (4), 800-808.

19. Larsen, A.; Stoltenberg, M.; West, M. J.; Danscher, G. Influence of bismuth on the number of neurons in cerebellum and hippocampus of normal and hypoxia-exposed mouse brain: a stereological study. *Journal of Applied Toxicology* **2005,** *25,* 383–392.

20. Mohan, R. Green bismuth. *Nature Chemistry,* April 2010, 336.

21. Marcillac, P. d.; Coron, N.; Dambier, G.; Leblanc, J.; Moalic, J.-P. Experimental detection of alpha-particles from the radioactive decay of natural bismuth. *Nature* **2003,** *422,* 876-878.

22. Rabin, O.; Perez, M.; Grimm, J.; Wojtkiewicz, G.; Weissleder, R. An X-ray computed tomography imaging agent based on long-circulating bismuth sulphide nanoparticles. *Nature Materials* **2006,** *5,* 118-122.

23. Metal Prices. Bismuth, 2015. MetalPrices. http://www.metalprices.com/p/BismuthFreeChart (accessed March 31, 2015).

24. Metal Prices. Metal Prices, 2015. Gold. www.metalprices.com/p/GoldFreeChart?weight=LB&size=M&theme=1011 (accessed March 31, 2015).

25. Goforth, A.; Brown, A. Bismuth particle x-ray contrast agents. US 20140194733 A1, July 10, 2014.

26. Aslan, K.; Wu, M.; Lakowicz, J. R.; Geddes, C. D. Fluorescent Core-Shell Ag@SiO2 Nanocomposites for Metal-Enhanced Fluorescence and Single Nanoparticle Sensing Platforms. *Journal of the American Chemical Society* **2007,** *129,* 1524-1525.

27. Garcia-Fuentes, M.; Torres, D.; Martin-Pastor, M.; Alonso, M. J. Application of NMR Spectroscopy to the Characterization of PEG-Stabilized Lipid Nanoparticles. *Langmuir* **2004,** *20,* 8839-8845.

28. NIST. National Institute of Standards and Technology. http://webbook.nist.gov/cgi/cbook.cgi?ID=C7732185&Type=IR-SPEC&Index=1#IR-SPEC (accessed August 4, 2014).

29. Shokri, B.; Abbasi Firouzjah, M.; Hosseini, S. I. FTIR analysis of silicon dioxide thin film deposited by Metal organic-based. *International Plasma Chemistry Society*, Antwerp, 2009; pp 1-4.